2006

Demonstration of Tunable Optical Notch Filter Using 1-D Opto-VLSI Processor

Chung Kiak Poh
Edith Cowan University

Kamal Alameh
Edith Cowan University

Zhenglin Wang
Edith Cowan University

10.1109/LPT.2006.875339
This is an Author's Accepted Manuscript of: Poh, C. K., Alameh, K. , & Wang, Z. (2006). Demonstration of Tunable Optical Notch Filter Using 1-D Opto-VLSI Processor. IEEE Photonics Technology Letters, 18(11), 1234-1236. Available here

Demonstration of Tunable Optical Notch Filter Using 1-D Opto-VLSI Processor

Chung-Kiak Poh, Kamal Alameh, *Senior Member, IEEE*, and Zhenglin Wang

***Abstract*—An opto-very-large-scale-integrated (opto-VLSI)-based tunable optical filter structure is demonstrated. Filter tunability is achieved by reconfiguring the holographic diffraction grating of an opto-VLSI processor, allowing virtually any type of filter response to be synthesized. A proof-of-concept tunable notch filter with wavelength span of 7 nm is experimentally verified.**

***Index Terms*—Opto-very-large-scale-integrated (opto-VLSI) processor, phase hologram, tunable notch filter.**

I. Introduction

TUNABLE optical filters are versatile devices that have applications in optical code-division multiple-access [1], [2], variable optical attenuators [3], space to wavelength switches [4], and dispersion compensators [5]. In particular, tunable optical notch filters are key components for spectral equalization in wavelength-division-multiplexing (WDM) optical networks [6], where the nonflat gain spectrum of erbium-doped fiber amplifiers (EDFA) leads to a power imbalance of the WDM channels, especially if many EDFAs are cascaded [7]. A dynamic gain-equalizer is also of great interest because the gain spectrum of the EDFA depends on its signal input power. Among potential technologies used for tunable notch filtering are mechanical switches [8], acoustooptic filters [9], and Fabry–Pérot filters [10]. Although these filter structures can tune the notch frequency, their ability to change the notch shape factor is limited.

In this letter, we report a dynamic optical notch filter employing an opto-very-large-scale-integrated (opto-VLSI) processor that generates dynamic digital diffraction gratings to perform adaptive spectral attenuation through optical beam steering. We experimentally demonstrate a tunable optical notch filter by reconfiguring the beam steering phase holograms of a one-dimensional (1-D) opto-VLSI processor. A computer algorithm is developed which optimizes the steering phase holograms that couple specific spectral wavebands to the output fiber port thus realizing a notch response with variable central wavelength and depth. A tuning range of 7 nm is demonstrated with a notch bandwidth of 1.2 nm and less than 1-dB passband ripples.

II. Theory

The key component of the tunable optical filter is the 1-D opto-VLSI processor. The opto-VLSI processor comprises an array of liquid crystal (LC) pixels that can be independently addressed by a VLSI circuit to reconfigure a multiphase hologram capable of beam steering and/or shaping [8]. By incorporating a thin quarter-wave plate layer between the LC and the VLSI backplane, a polarization-insensitive opto-VLSI processor can be realized, allowing optical beam steering with polarization-dependent loss as low as 0.5 dB [9].

The application of a periodic sequence of voltage ramps of period Λ across the opto-VLSI array aperture steers the incident light beam to an angle θ (relative to the normal) given by the general grating equation [10]

$$\theta = \sin^{-1}\left[\frac{\lambda_o}{\Lambda} - \sin(\theta_{\rm inc})\right] \tag{1}$$

where λ_o is the incident wavelength in free space, $\theta_{\rm inc}$ is the angle of incidence relative to the normal, $\Lambda = q \times d$ is the grating period, q is the number of pixels within the grating period, and d is the center-to-center spacing between the pixels.

The steering angle θ depends on the periodicity (and sign) of the applied voltage ramp. Current LC materials suffer from fringing field and resistance to rapid change in orientation and as a consequence, a portion of the incident wavefront is steered to the wrong angle, resulting in a loss in the correct direction and high sidelobes [10]. The overall steering efficiency $\eta_{\rm overall}$ is given by [10]

$$\eta_{\rm overall} = \left[\frac{\sin(\pi/q)}{\pi/q}\right]^2 \cdot \left(1 - \frac{\Lambda_F}{q \cdot d}\right)^2 \tag{2}$$

where Λ_F is the width of the flyback region. It is important to note that the overall steering efficiency can be increased by increasing the number of pixels within a grating period. However, this reduces the maximum steering angle as obvious from (1).

III. Tunable Optical Filter Architecture

The architecture of the tunable optical filter is as shown in Fig. 1. It consists of a circulator, fiber collimator, a diffraction grating, and a 1-D opto-VLSI processor. The diffraction grating maps the different wavebands of the collimated input optical signal onto different pixel blocks on the active area of the opto-VLSI processor. By driving each pixel block with the appropriate hologram, a waveband in that region can either be steered back along the incidence path, thus coupling it into the fiber collimator with minimum attenuation, or deliberately steered "off-track" so that its power is partially coupled back into the fiber collimator leading to a high optical attenuation for that waveband component. By optimizing the phase holograms of the pixel blocks, one can control the overlapping between the

Manuscript received November 16, 2005; revised February 25, 2006.
The authors are with the WA Centre of Excellence for Microphotonic Systems, Edith Cowan University, Joondalup, WA 6027 Australia (e-mail: chungp@student.ecu.edu.au; k.alameh@ecu.edu.au).
Digital Object Identifier 10.1109/LPT.2006.875339

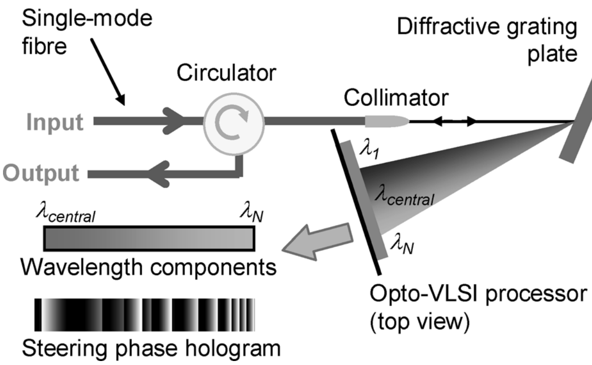

Fig. 1. Reconfigurable optical notch filter architecture. The pixels are partitioned into pixel blocks; each has a different phase hologram that steers incident wavebands from λ_{central} to λ_N back into the collimator.

coupled waveband leading to a notch filter response with low passband ripples.

IV. Results and Discussion

An erbium amplified spontaneous emission source was used to generate a broadband input optical signal of uniform spectrum, which was routed, through the circulator, to the fiber collimator and collimated at 1-mm diameter, as shown in Fig. 1. The diffraction grating used in the experiments was a blazed grating of 1200 lines/mm and the 1-D opto-VLSI processor had 1×4096 pixels. The maximum voltage applied to the pixels was ± 5 V. The opto-VLSI processor used in the experiments had a low reflectivity and a low fill factor resulting in a measured insertion loss of about 6–11 dB depending on the steering angle. The measured two-way fiber coupling losses were around 2 dB. A program was written in LabVIEW to generate and send command voltages in the form of 1-D image to the opto-VLSI processor to generate optimized steering holograms for the incident wavebands. The program allowed the user to create as many input channels as required, with each channel independently controlled in terms of position, width, and phase profile. The default (or initial) phase hologram used for the real-time optimization procedure was a blazed grating. The steered wavebands were coupled into the fiber and routed via the circulator to the output port and monitored by an optical spectrum analyzer.

The first part of the experiment focused on the generation of a flat passband filter. Multiple independent holograms with different widths and periods were optimized in real-time to synthesize a flat passband response with 7-nm bandwidth and a ripple level less than 1 dB. This is shown in Fig. 2(b) as graph H_1 whose corresponding hologram is shown in Fig. 2(a). The limited bandwidth was due to the limited active area of the opto-VLSI processor, which was around 6 mm. It was found that the width of a pixel block influences the reflected power coupled into the fiber collimator and hence controls the attenuation of the waveband associated to that pixel block. It was also found that the position of the pixel block relative to the center of the associated waveband influences the bandwidth and sidelobes of the coupled wavebands. Note that, by using an opto-VLSI processor with wider active window or diffraction grating with lower groove frequency, a broader tuning wavelength span can be achieved.

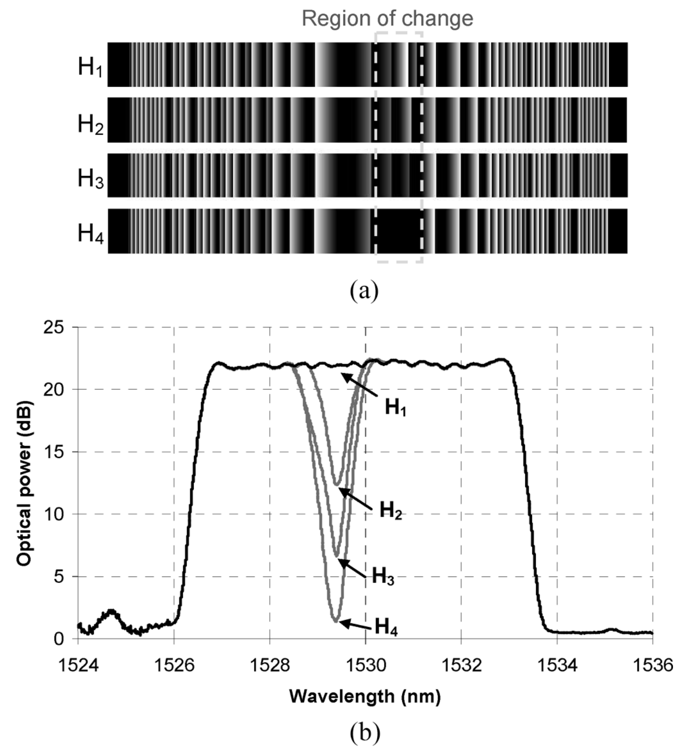

Fig. 2. (a) Holograms in the form of 1-D digital image for the flat-passband and the various notch filter responses. H_1: Hologram for the flat passband; H_2: Hologram for the notch filter with 10-dB attenuation; H_3: Hologram for the notch filter with 15-dB attenuation; and H_4: Hologram for the notch filter with 20-dB attenuation. (b) Various filter responses that correspond to input hologram from H_1 to H_4. The notches are centered around 1529.5 nm.

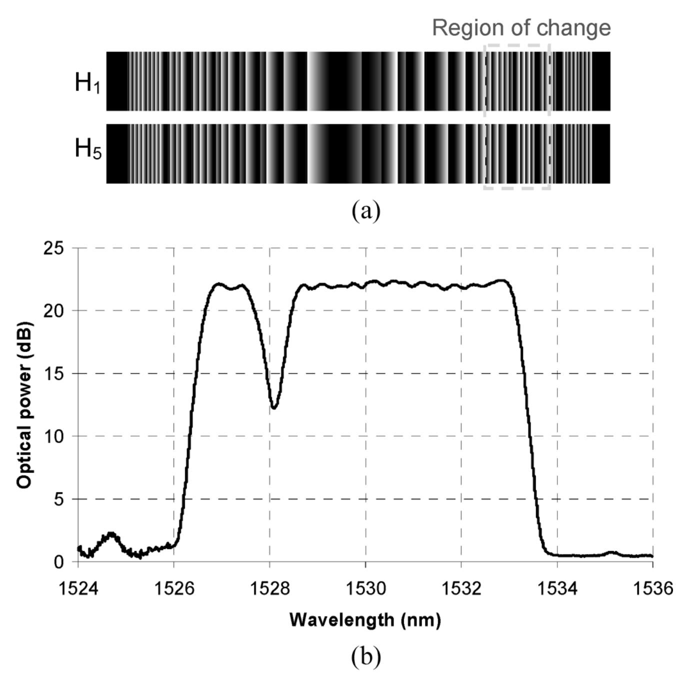

Fig. 3. (a) H_5: Hologram used to generate the 10-dB notch filter centered at 1528.1 nm. Changes in the hologram relative to H_1 are highlighted. (b) A 10-dB-deep notch filter response centered at 1528.1 nm generated using hologram H_5.

The second part of the experiments concentrated on the demonstration of a reconfigurable notch filter response. A notch was inserted at 1529.5 nm and was attenuated by 10, 15,

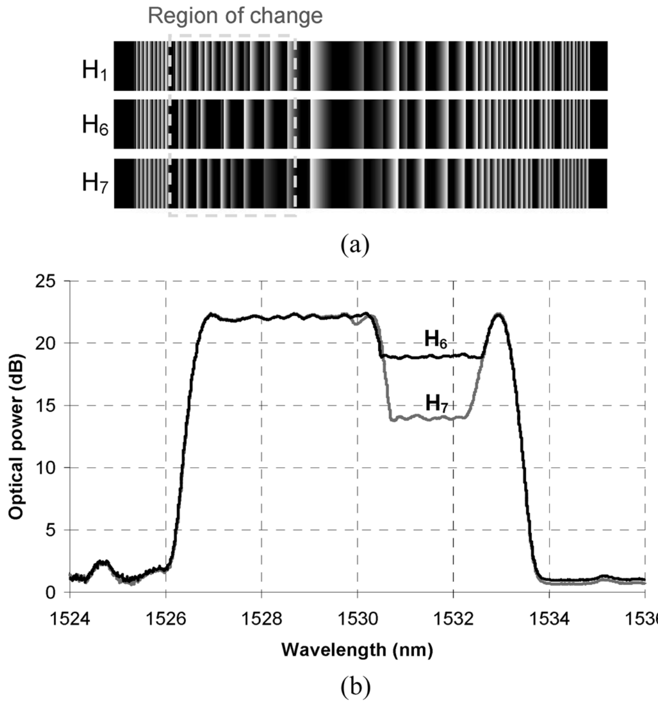

Fig. 4. (a) Holograms used to generate the flat notch responses. Hologram H_1 is included for comparison. H_6: Hologram for the flat notch with 3-dB attenuation and a 3-dB bandwidth of 2 nm; and H_7: Hologram for the flat notch with 8-dB attenuation and a 3-dB bandwidth of 1.5 nm. (b) Flat notch response with variable attenuation generated using hologram H_6 and H_7.

and 20 dB with respect to the passband level while keeping the ripple level to within 1 dB, as shown in Fig. 2(b), where graphs are labeled according to their corresponding phase holograms H_2 to H_4 that are shown in Fig. 2(a). It is obvious from Fig. 2(a) and (b) that the notch depth can be controlled by changing the phase profile of a small pixel group [highlighted in Fig. 2(a)] while keeping the rest of the hologram intact.

Since the passband was constructed by a series of independent phase holograms, it was also possible to have the notch centered at any wavelength (within the passband limit) with arbitrary notch bandwidth and depth, as shown in Fig. 3(b) whose corresponding phase hologram H_5 is shown in Fig. 3(a). Also highlighted for comparison is the hologram H_1 that was used to generate the flat passband response.

Fig. 4(a) and (b) shows the holograms that generate flat notch responses of bandwidth 2 nm centered around 1531.5 nm. The flat notch depth could be varied from 3 to 8 dB simply by adjusting the input phase hologram of the pixel blocks corresponding to the flat notch region [Fig. 4(a)]. This validates the potential of opto-VLSI technology to generate arbitrary optical notch filter responses.

V. Conclusion

We have demonstrated a reconfigurable optical notch filter based on a 1-D opto-VLSI processing. The ability to control the bandwidth, central frequency, and depth of the notch filter has been demonstrated over a 7-nm wavelength span with less than 1 dB of passband ripples.

References

[1] A. Weiner, “Femtosecond pulse shaping using spatial light modulators,” *Rev. Sci. Instrum.*, vol. 71, pp. 1929–1960, 2000.

[2] H. P. Sardesai, C. C. Chang, and A. M. Weiner, “A femtosecond code division multiple access communication system test bed,” *J. Lightw. Technol.*, vol. 16, no. 11, pp. 1953–1964, Nov. 1998.

[3] J. E. Ford and J. A. Walker, “Dynamic spectral power equalization using micro-opto-mechanics,” *IEEE Photon. Technol. Lett.*, vol. 10, no. 10, pp. 1440–1442, Oct. 1998.

[4] D. T. Fuchs, C. R. Doerr, V. A. Aksyuk, M. E. Simon, L. W. Stulz, S. Chandrasekhar, L. L. Buhl, M. Cappuzzo, L. Gomez, A. Wong-Foy, E. Laskowski, E. Chen, and R. Pafchek, “A hybrid MEMS-waveguide wavelength selective crossconnect,” *IEEE Photon. Technol. Lett.*, vol. 16, no. 1, pp. 99–101, Jan. 2004.

[5] T. Sano, T. Iwashima, M. Katayama, T. Kanie, M. Harumoto, M. Shigehara, H. Suganuma, and M. Nishimura, “Novel multichannel tunable chromatic dispersion compensator based on MEMS and diffraction grating,” *IEEE Photon. Technol. Lett.*, vol. 15, no. 8, pp. 1109–1110, Aug. 2003.

[6] K. Maru, K. Tanaka, T. Chiba, H. Nonen, and H. Uetsuka, “Dynamic gain equalizer using proposed adjustment procedure for thermooptic phase shifters under the influence of thermal crosstalk,” *J. Lightw. Technol.*, vol. 22, no. 6, pp. 1523–1532, Jun. 2004.

[7] S. Wada, S. Abe, Y. Ota, B. Reichman, T. Imura, and C. A. Daza, “Variable gain equalizer using magneto-optics,” in *Optical Fiber Communication Conf. Exhibit (OFC)*, 2002, pp. 324–326.

[8] R. Giles, V. Aksyuk, and B. Barber, “A silicon MEMS optical switch attenuator and its use in lightwave subsystems,” *IEEE J. Sel. Topics Quantum Electron.*, vol. 5, no. 1, pp. 18–25, Jan. 1999.

[9] J. L. Jackel, J. L. Goodman, M. S. Baran, and J. E. Tomlinson, “Acousto-optic tunable filters (AOTFs) for multiwavelength optical cross-connects: crosstalk considerations,” *J. Lightw. Technol.*, vol. 14, no. 6, pp. 1056–1066, Jun. 1996.

[10] D. Sadot and E. Boimovich, “Tunable optical filters for dense WDM networks,” *IEEE Commun. Mag.*, vol. 36, no. 12, pp. 50–55, Dec. 1998.

[11] M. Raisi, S. Ahderom, K. E. Alameh, and K. Eshraghian, “Opto-VLSI multiband tunable optical filter,” *Electron. Lett.*, vol. 39, no. 21, pp. 1533–1534, Oct. 2003.

[12] I. G. Manolis, T. D. Wilkinson, M. M. Redmond, and W. A. Crossland, “Reconfigurable multilevel phase holograms for Optical switches,” *IEEE Photon. Technol. Lett.*, vol. 4, no. 6, pp. 801–803, Jun. 2002.

[13] P. McManamon, T. A. Dorschner, and D. L. Corkum, “Optical Phased Array Technology,” *IEEE Proc.*, vol. 84, no. 2, pp. 268–298, Feb. 1996.